Supporting Information for

A diphosphoramidite ligand for hydroformylation of various olefins

Cheng Li,[a] Siqi Li,[a] Haoran Liang,*[a] Haiyan Fu,*[b] and Hua Chen[b]

[a] *Chongqing Key Lab of Medicinal Chemistry & Molecular Pharmacology, School of Pharmacy and Bioengineering, Chongqing University of Technology, Chongqing 400054, P. R. China*
[b] *Key Laboratory of Green Chemistry & Technology, Ministry of Education, College of Chemistry, Sichuan University, Chengdu 610064, P. R. China*

Table of Contents

1. General Information

Unless otherwise stated, commercial reagents were used without purification. All manipulations of air- and moisture-sensitive reagents were performed under an inert atmosphere of argon in either a vacuum atmosphere or using standard Schlenk techniques. ^{1}H, ^{13}C and ^{31}P NMR spectra were recorded on Bruker AVANCE III HD-400 MHz NMR spectrometers. Multiplets were assigned as s (singlet), d (doublet), t (triplet), and m (multiplet). High resolution mass spectra (HRMS) were recorded with a Shimadzu LCMS-IT-TOF high resolution liquid chromatograph. GC analysis was performed on an Agilent 8860 chromatograph (KB-5, 30m*320um*0.25um, FID). GC conditions: 70 °C for 5 min, then 290 °C for 12 min (rate 15 °C/min). GC-MS analysis was conducted on a SHIMADZU GCMS-QP2010SE (KB-5MS, 30 m*0.25 mm*0.25 μm). Melting points were obtained by X-4B micro Melting Point Measurement Instrument.

2. Preparation and Spectral Data of Ligand

The ligand backbone 1,1′-bis-(6,7,8,9-tetrahydro-2-hydroxy-dibenzofuran) was prepared based on the literature.[1]

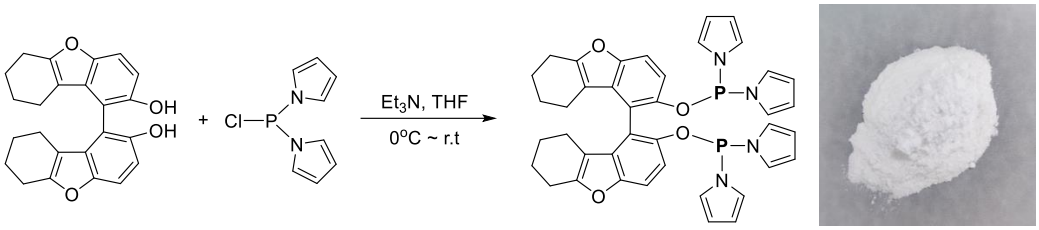

A solution of pyrrole (6.9 mL, 100 mmol) in THF (20 mL) was added dropwise to a solution of phosphorus trichloride (4.4 mL, 50 mmol) and triethylamine (20 mL, 144 mmol) in THF (100 mL) at 0 °C under argon atmosphere. A white precipitate generated immediately upon addition. The reaction mixture was stirred overnight at room temperature. The reaction mixture was used directly in the next reaction. A solution of 1,1′-bis-(6,7,8,9-tetrahydro-2-hydroxy-dibenzofuran) (4.49 g, 12 mmol) in THF (30 mL) was added dropwise to a former solution of chlorodipyrrolylphosphine and another of triethylamine (10 mL, 72 mmol) at 0 °C under argon atmosphere. The reaction mixture was stirred overnight at room temperature. The triethylamine•HCl salts were filtered off at room temperature once the reaction was accomplished. The solvent was subsequently removed under diminished pressure, and the residue was purified via recrystallization with ethanol to obtained desired compound as a white solid (5.66 g, 67.6%).

M.p.: 132-134 °C.

HRMS (ESI+): calcd for $C_{40}H_{36}N_4O_4P_2$: 698.2212; found: 699.2128.

^{1}H NMR (400 MHz, $CDCl_3$) δ 7.28 (d, J = 8.7 Hz, 2H), 6.75 (d, J = 8.7 Hz, 2H), 6.63 – 6.55 (m, 8H), 6.19 – 6.10 (m, 8H), 2.66 (t, J = 6.0 Hz, 4H), 1.89 – 1.64 (m, 8H), 1.56 – 1.45 (m, 4H) ppm.

^{13}C NMR (101 MHz, $CDCl_3$) δ 156.02, 150.60, 146.74, 129.88, 121.09, 118.42, 114.29, 113.64, 111.92, 111.00, 23.61, 22.53, 22.37, 20.53 ppm.

^{31}P NMR (162 MHz, $CDCl_3$) δ 109.39 ppm.

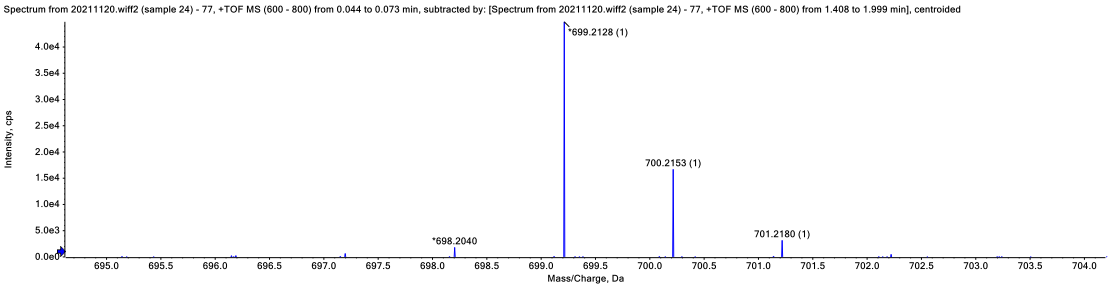

Figure S1. HRMS(ESI+) spectra of pyTFBP

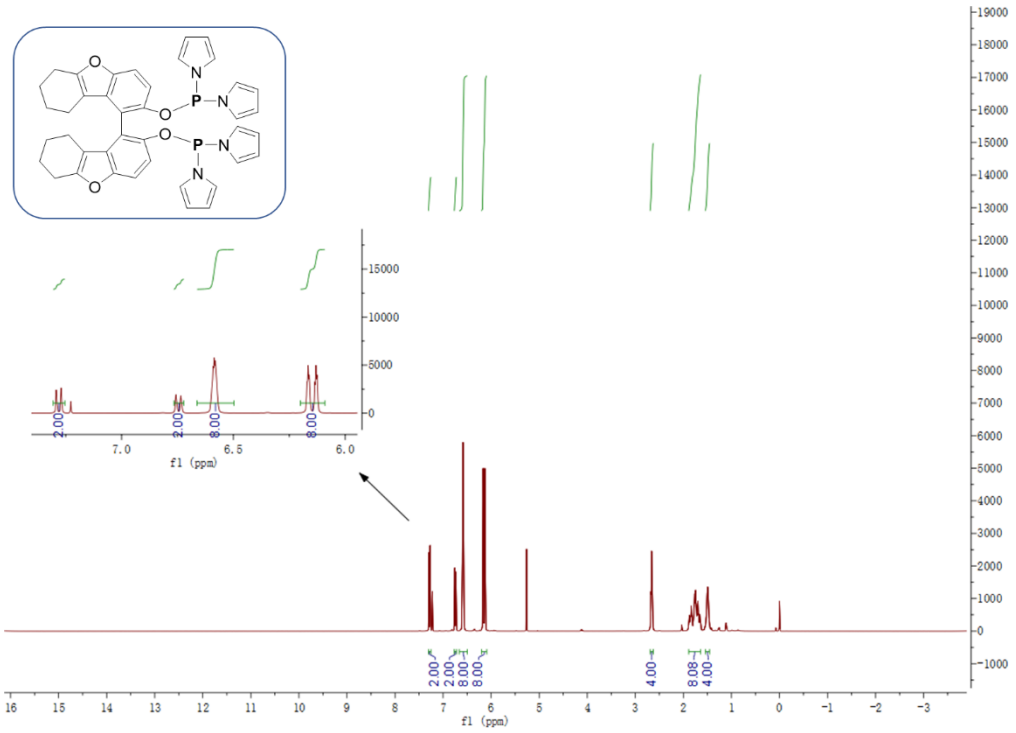

Figure S2. ^{1}H NMR spectra of pyTFBP in $CDCl_3$

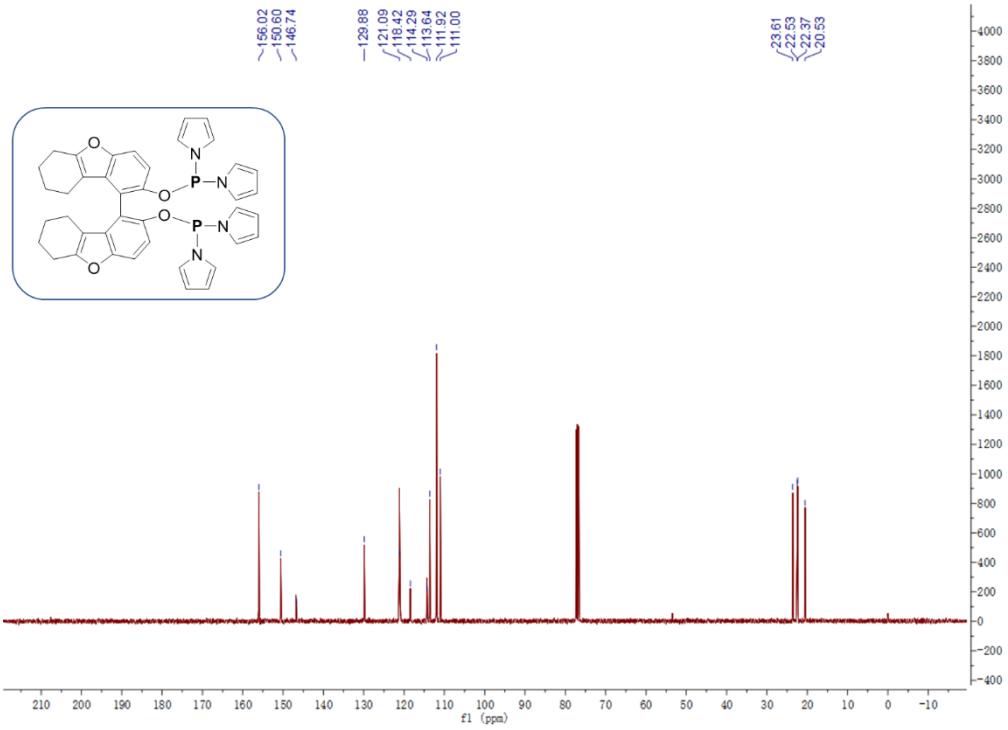

Figure S3. ^{13}C NMR spectra of pyTFBP in $CDCl_3$

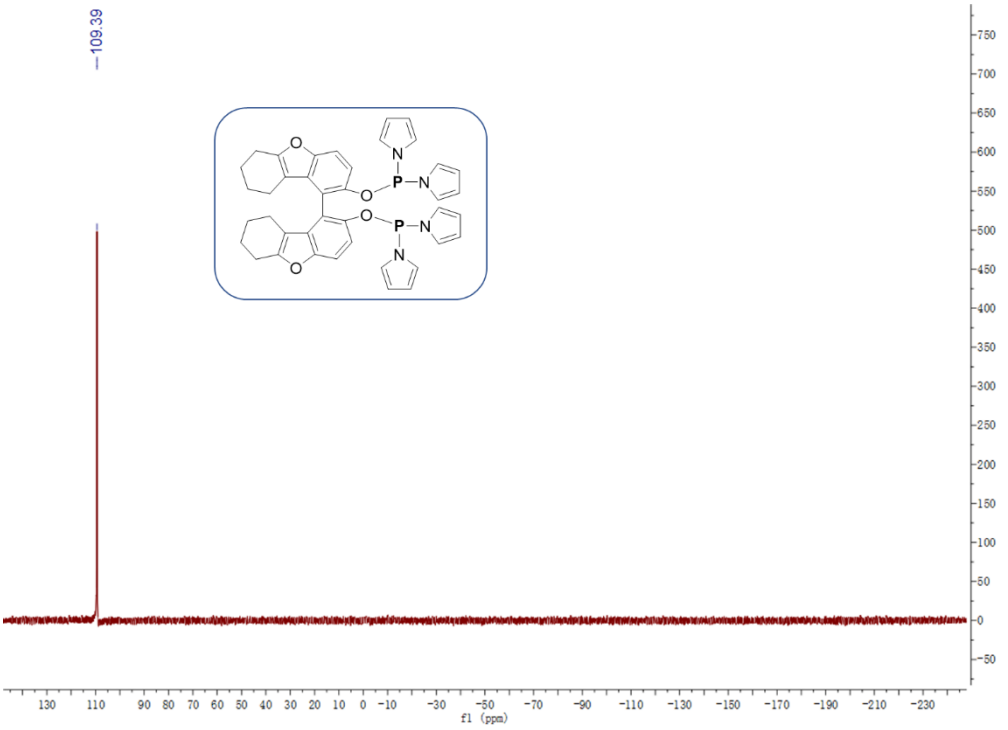

Figure S4. ^{31}P NMR spectra of pyTFBP in $CDCl_3$

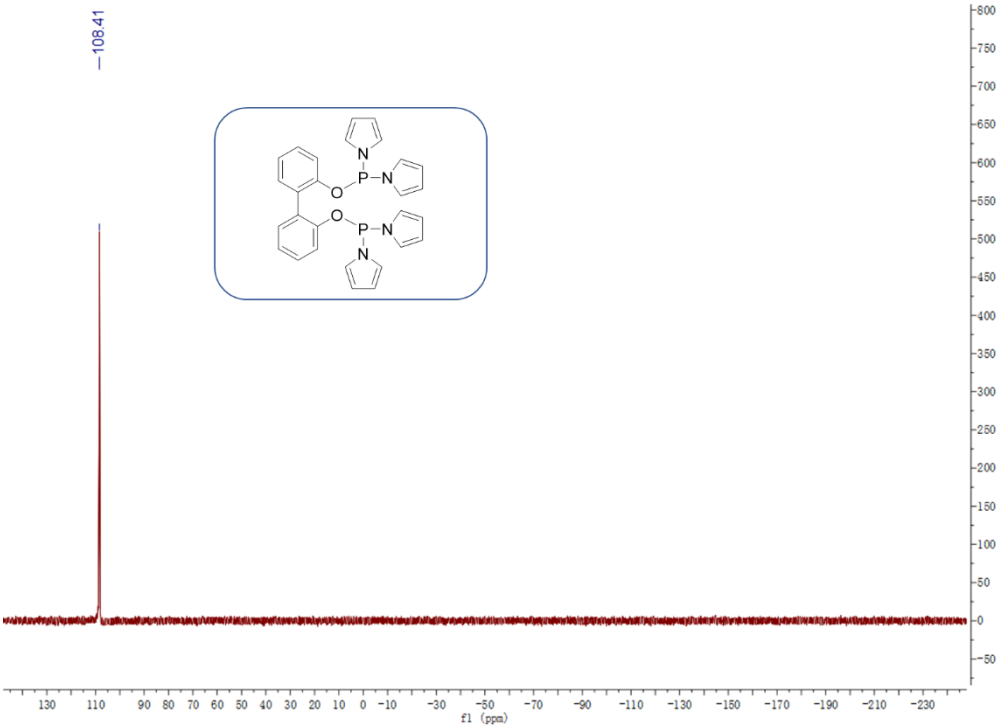

Figure S5. ^{31}P NMR spectra of pyBP in $CDCl_3$

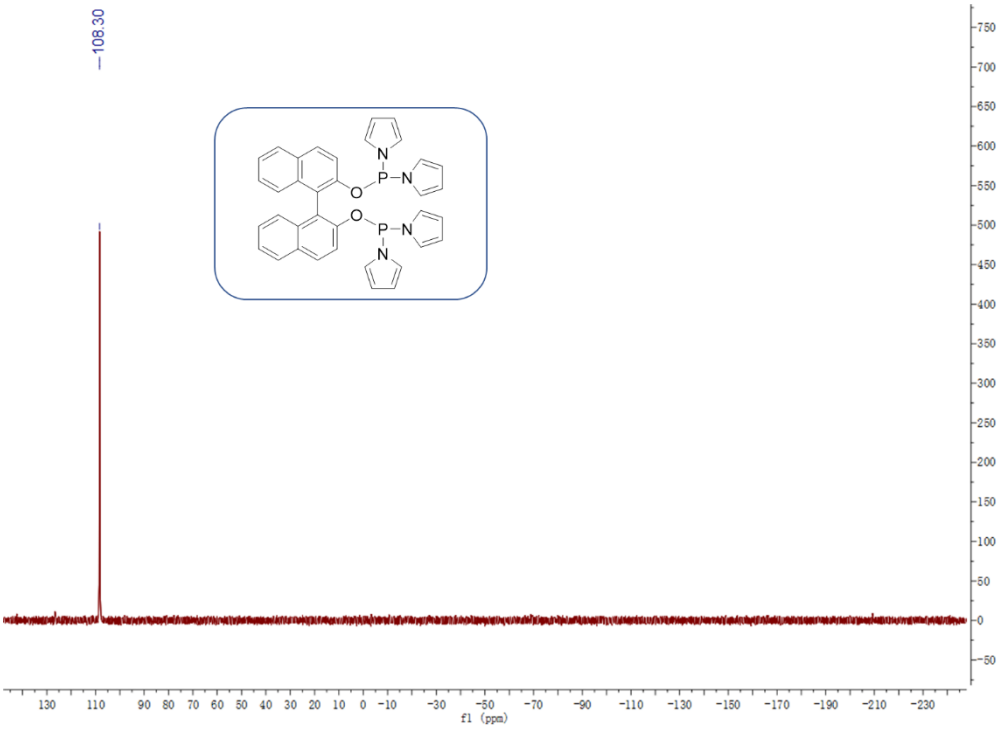

Figure S6. ^{31}P NMR spectra of pyBN in $CDCl_3$

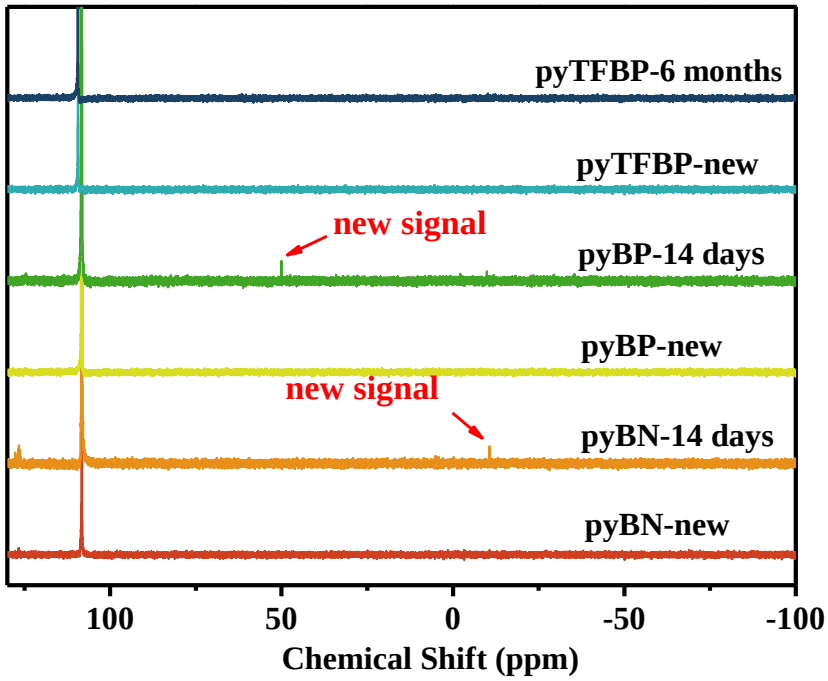

Figure S7. Comparison of the ^{31}P NMR spectra

3. Preparation and Spectral Data of Crotonaldehyde Ethylene Acetal

Crotonaldehyde ethylene acetal was prepared based on the literature.[2] The anticipated structure has been confirmed by GC-MS and ^{1}H NMR spectra, which is consist with the literature.

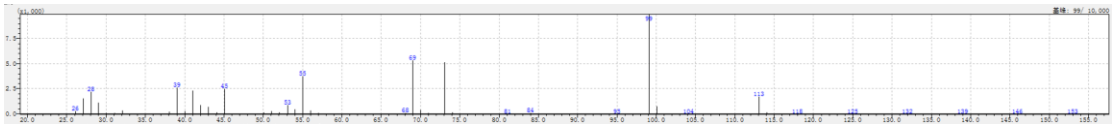

Figure S8. GC-MS of crotonaldehyde ethylene acetal

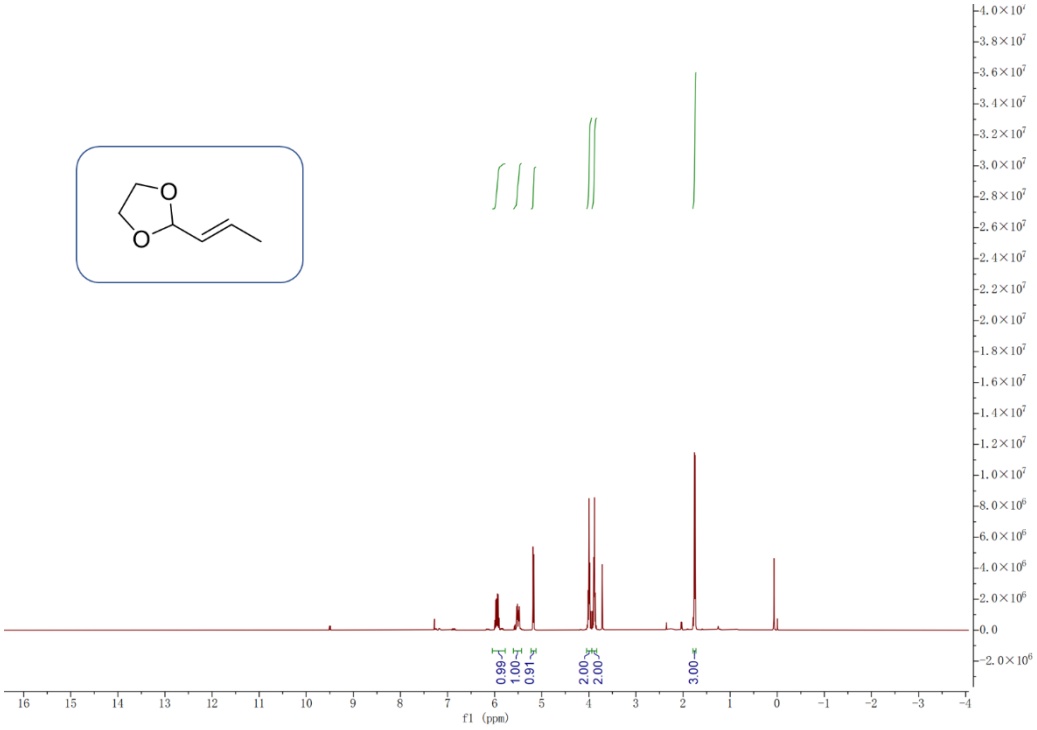

Figure S9. ^{1}H NMR spectra of crotonaldehyde ethylene acetal in $CDCl_3$

4. General Information for the Hydroformylation Reaction

The hydroformylation reaction was conducted in a 25 mL or 50 mL high-pressure autoclave. In a typical run, precatalyst, ligand and substrate were loaded. And then the reactor was purged with syngas, and charged with high-pressure syngas. The reactor was heated to the desired temperature with stirring. After the reaction time, the autoclave was cooled quickly in an ice-water bath, and then vented slowly. The reaction products were determined by GC-MS and quantified by GC.

5. Optimization for Hydroformylation of Olefins

Table S1. Optimization for hydroformylation of 2-pentene[a]

Entry	T[°C]	L/Rh	CO/H_2[MPa]	TON[b]	$Sel._{CHO}$[c][%]	Linear[d][%]	*l*/*b*[e]
1	100	1	1.0	392	93.1	43.1	0.8
2	100	2	1.0	781	98.2	79.8	3.9
3	100	3	1.0	983	94.6	91.5	10.7
4	100	4	1.0	984	94.7	96.4	26.7
5	100	5	1.0	988	94.4	96.2	25.0
6	80	4	1.0	785	99.3	97.0	32.4
7	90	4	1.0	897	98.5	97.0	32.8
8	90	4	0.5	877	97.6	97.0	32.2
9	90	4	2.0	938	97.8	97.1	33.3

[a] Reaction conditions: S/C=1000, 2-pentene (14.6 mmol), $[Rh(CO)_2(acac)]$(2.9 mM in xylene, 5.0 mL), 2 h, decane (0.2 mL) as internal standard. [b] Turnover number, determined on the basis of alkene conversion by GC analysis. [c] Percentage of aldehyde in all products. [d] Percentage of linear aldehyde in all aldehydes. [e] Linear/branched ratio.

Table S2. Optimization for hydroformylation of 2-octene[a]

Entry	T[°C]	L/Rh	CO/H_2[MPa]	TON[b]	$Sel._{CHO}$[c][%]	Linear[d][%]	*l*/*b*[e]
1	90	2	1.0	809	60.2	51.3	1.1
2	90	3	1.0	827	60.3	85.0	5.7
3	90	4	1.0	852	63.1	98.4	63
4	90	5	1.0	845	64.0	98.1	52.5
5	80	4	1.0	714	63.8	98.7	78.7
6	100	4	1.0	895	70.6	98.0	48.9
7	110	4	1.0	905	70.8	96.9	31.2
8	100	4	0.5	830	57.6	97.8	44.8
9	100	4	2.0	930	77.4	98.1	51.3
10	100	4	3.0	934	77.8	97.2	34.9
11[f]	100	24	2.0	8360	62.4	97.8	44.0

[a] Reaction conditions: S/C=1000, 2-octene (14.6 mmol), $[Rh(CO)_2(acac)]$(2.9 mM in toluene, 5.0 mL), 2 h, decane (0.2 mL) as internal standard. [b-e] See Table S1. [f] S/C=10000.

Table S3. Optimization for hydroformylation of methyl acrylate[a]

Entry	T[°C]	L/Rh	CO/H_2[MPa]	TON[b]	$Sel._{CHO}$[c][%]	Linear[d][%]	*l*/*b*[e]
1	100	1	1.0	11280	83.8	93.9	15.3
2	100	2	1.0	14460	83.2	94.7	17.8
3	100	3	1.0	15580	84.0	95.9	23.4
4	100	4	1.0	14340	81.0	93.7	14.9
5	60	3	1.0	12800	51.5	51.2	1.1
6	80	3	1.0	17840	68.0	80.4	4.1
7	120	3	1.0	13300	71.9	96.2	25.6
8	100	3	0.5	11800	82.8	96.7	29.7
9	100	3	2.0	17780	66.1	83.5	5.0

[a] Reaction conditions: S/C=20000, methyl acrylate (100 mmol), $[Rh(CO)_2(acac)]$(1.0 mM in toluene, 5.0 mL), 2 h,

decane (0.2mL) as internal standard. [b-e] See Table S1.

Table S4. Optimization for hydroformylation of allyl acetate[a]

Entry	T[°C]	L/Rh	CO/H_2[MPa]	TON[b]	Sel.$_{CHO}$[c][%]	Linear[d][%]	*l*/*b*[e]
1	100	3	1.0	5440	85.5	82.5	4.7
2	100	4	1.0	8810	87.8	85.1	5.7
3	100	5	1.0	9250	88.1	87.5	7.0
4	100	6	1.0	9290	96.7	80.5	4.1
5	100	7	1.0	8710	93.3	75.8	3.1
6	60	5	1.0	9660	97.4	75.4	3.1
7	80	5	1.0	9740	98.9	86.2	6.3
8	120	5	1.0	7420	71.3	87.7	7.1
9	80	5	0.5	8530	94.5	85.8	6.0
10	80	5	2.0	9860	98.2	79.9	4.0

[a] Reaction conditions: S/C=10000, allyl acetate (146 mmol), [$Rh(CO)_2(acac)$](2.9 mM in toluene, 5.0 mL), 2 h, dodecane (0.2mL) as internal standard. [b-e] See Table S1.

Table S5. Optimization for hydroformylation of crotonaldehyde ethylene acetal[a]

Entry	T[°C]	L/Rh	CO/H_2[MPa]	TON[b]	Sel.$_{CHO}$[c][%]	Linear[d][%]	*l*/*b*[e]
1	100	4	1.0	1172	95.9	89.3	8.3
2	100	5	1.0	1266	94.9	90.6	9.6
3	100	6	1.0	1338	95.1	91.7	11.0
4	100	7	1.0	1752	96.8	93.9	15.4
5	100	8	1.0	1864	96.9	95.1	19.4
6	80	8	1.0	720	94.1	87.1	6.7
7	120	8	1.0	1866	94.4	93.9	15.4
8	100	8	2.0	1464	87.0	85.2	5.8
9	100	8	0.5	1766	96.1	95.7	22.3

[a] Reaction conditions: S/C=2000, crotonaldehyde ethylene acetal (29.2 mmol), [$Rh(CO)_2(acac)$](2.9 mM in toluene, 5.0 mL), 1 h, decane (0.2mL) as internal standard. [b-e] See Table S1.

Table S6. Optimization for hydroformylation of styrene[a]

Entry	T[°C]	L/Rh	CO/H_2[MPa]	TON[b]	Sel.$_{CHO}$[c][%]	Linear[d][%]	*l*/*b*[e]
1	80	1	2.0	10660	96.6	63.7	1.8
2	80	2	2.0	11800	98.7	63.6	1.7
3	80	3	2.0	18640	99.9	82.7	4.8
4	80	4	2.0	18060	99.8	83.5	5.1
5	80	3	1.0	18660	96.9	85.7	6.0
6	80	3	0.5	13120	96.3	87.0	6.7
7	100	3	1.0	19900	95.8	85.9	6.1
8	120	3	1.0	18420	89.3	84.6	5.5
9[f]	100	3	1.0	38200	95.5	85.8	6.1

[a] Reaction conditions: S/C=20000, styrene (100 mmol), [$Rh(CO)_2(acac)$](1.0 mM in toluene, 5.0 mL), 1 h, decane (0.2mL) as internal standard. [b-e] See Table S1. [f] S/C = 40000.

6. GC and GC-MS Results of Hydroformylation Reactions

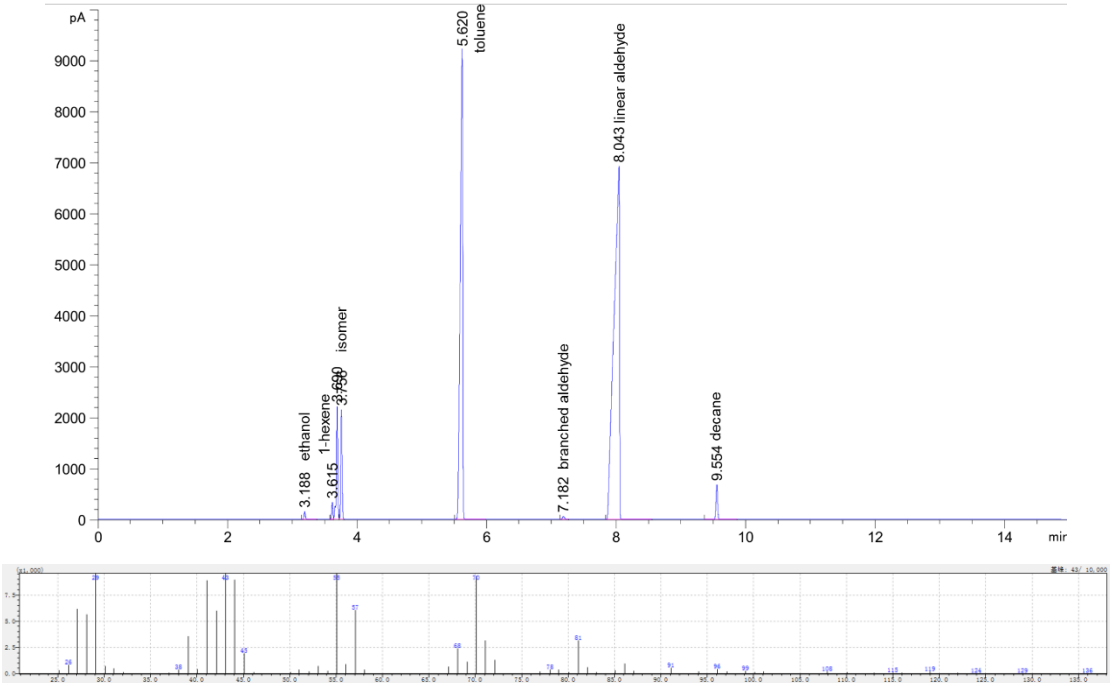

Figure S10. GC of 1-hexene hydroformylation and GC-MS of 1-heptaldehyde

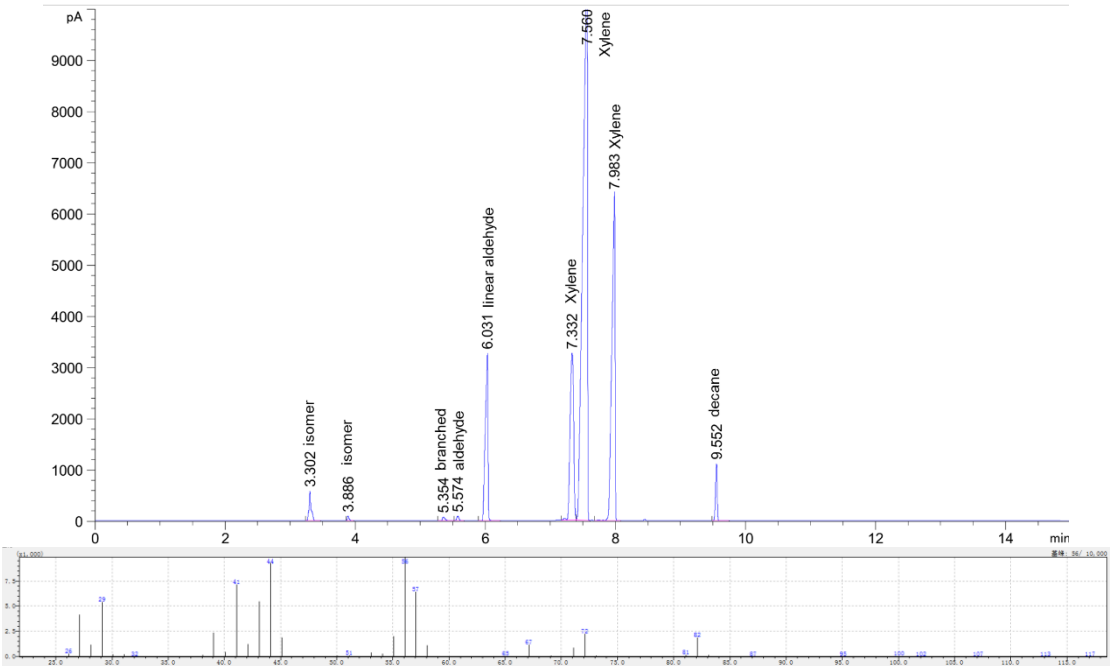

Figure S11. GC of 2-pentene hydroformylation and GC-MS of 1-hexaldehyde

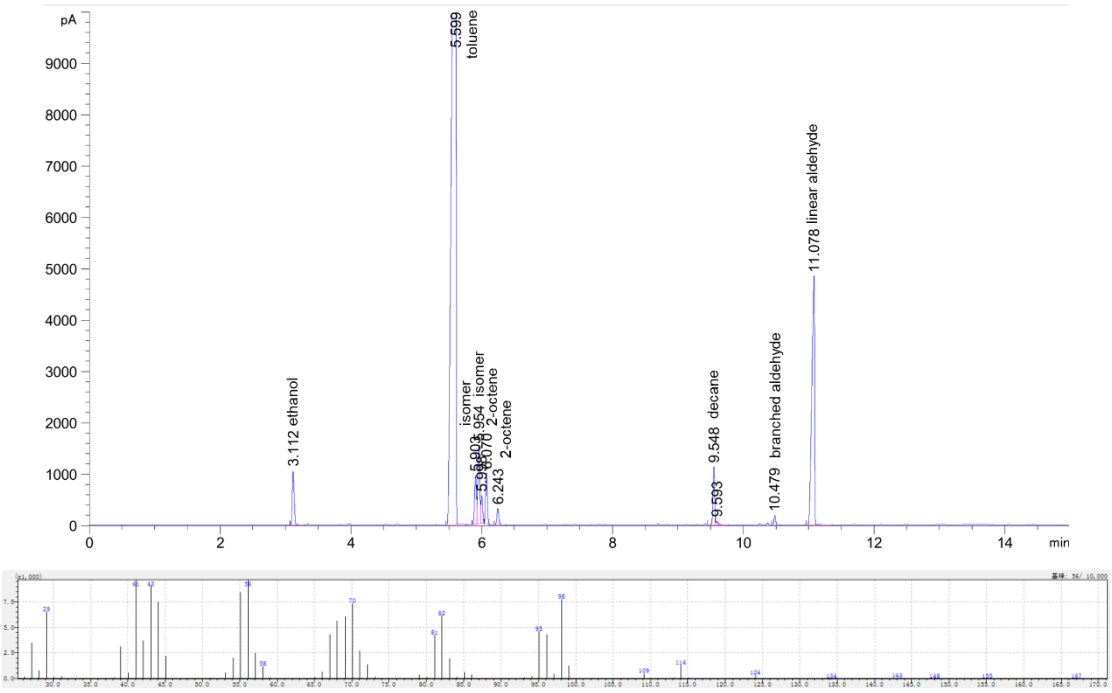

Figure S12. GC of 2-octene hydroformylation and GC-MS of 1-nonanaldehyde

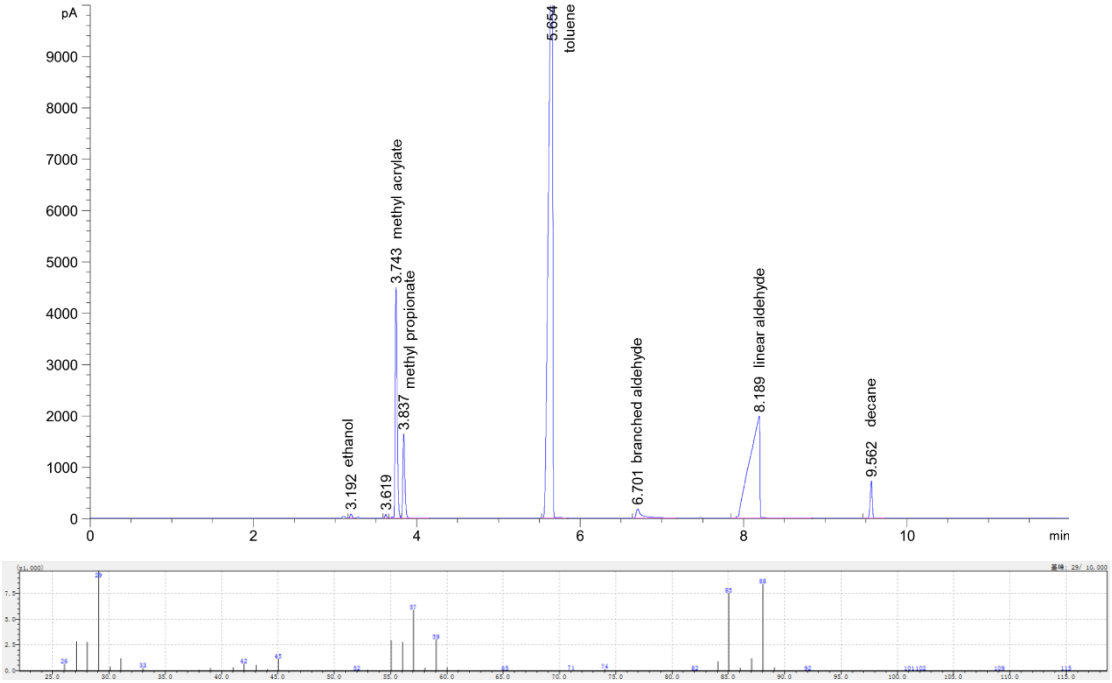

Figure S13. GC of methyl acrylate hydroformylation and GC-MS of corresponding linear aldehyde

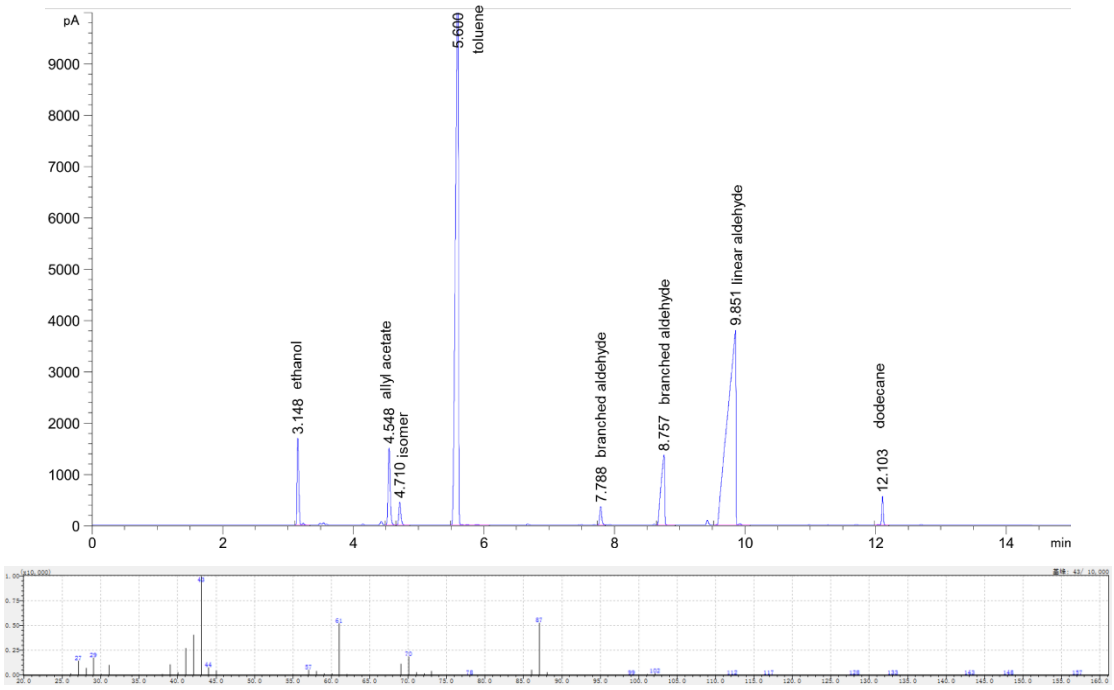

Figure S14. GC of allyl acetate hydroformylation and GC-MS of corresponding linear aldehyde

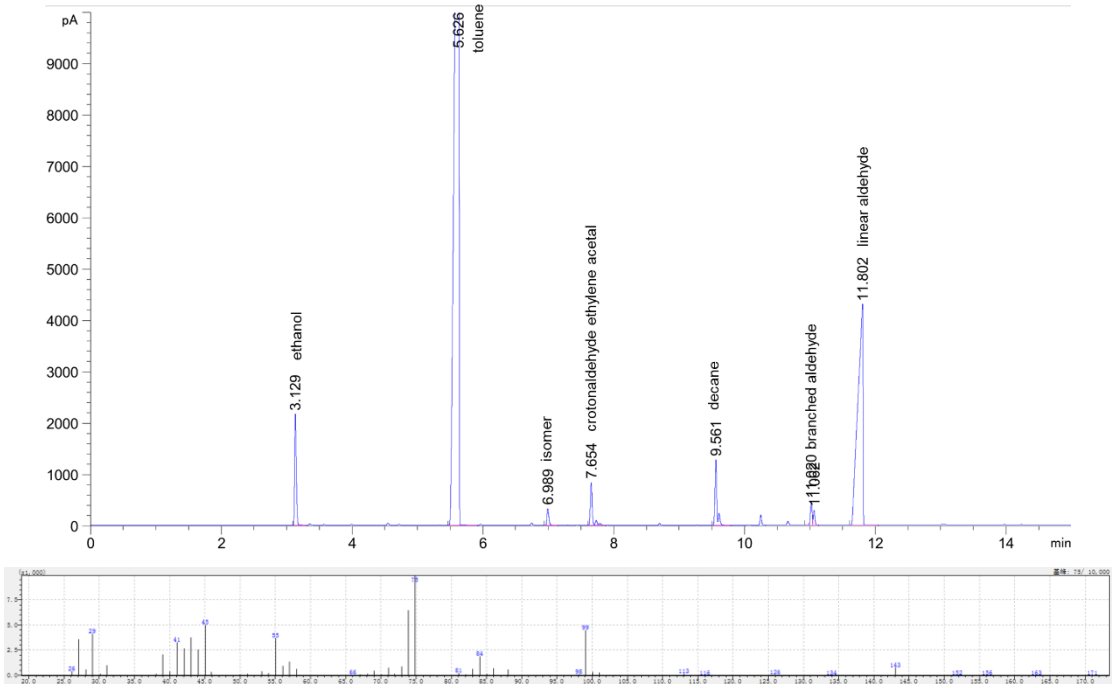

Figure S15. GC of crotonaldehyde ethylene acetal hydroformylation and GC-MS of corresponding linear aldehyde

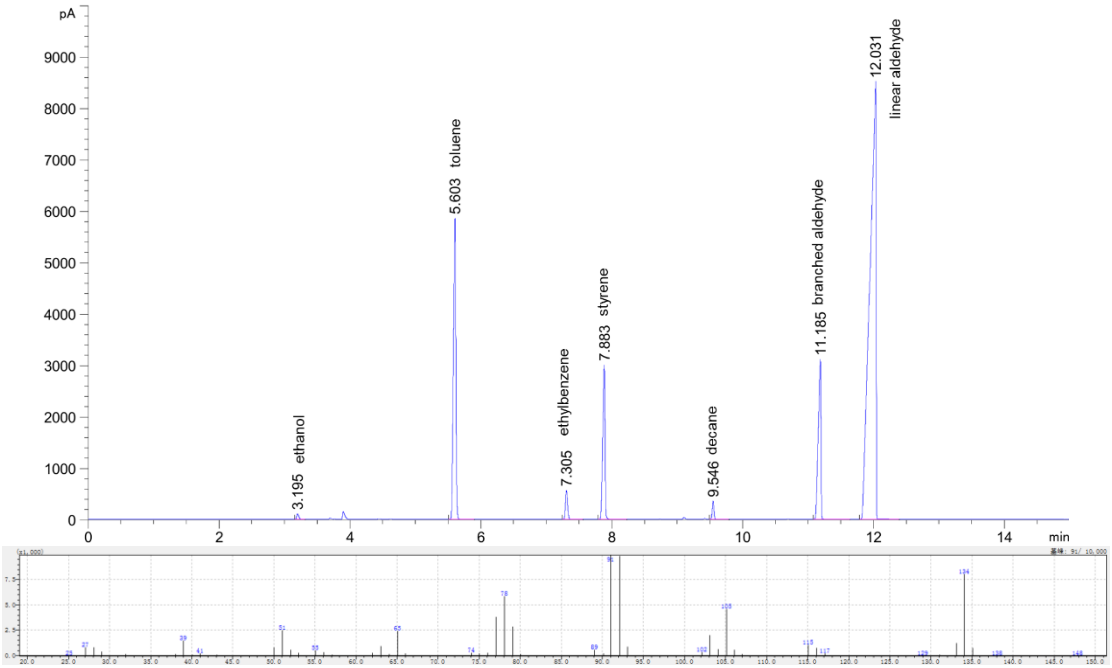

Figure S16. GC of styrene hydroformylation and GC-MS of corresponding linear aldehyde

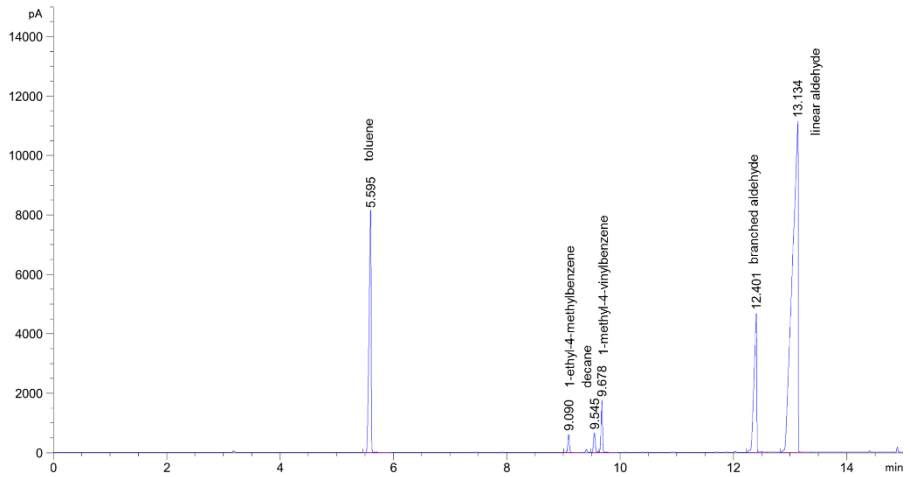

Figure S17. GC of 1-methyl-4-vinylbenzene hydroformylation

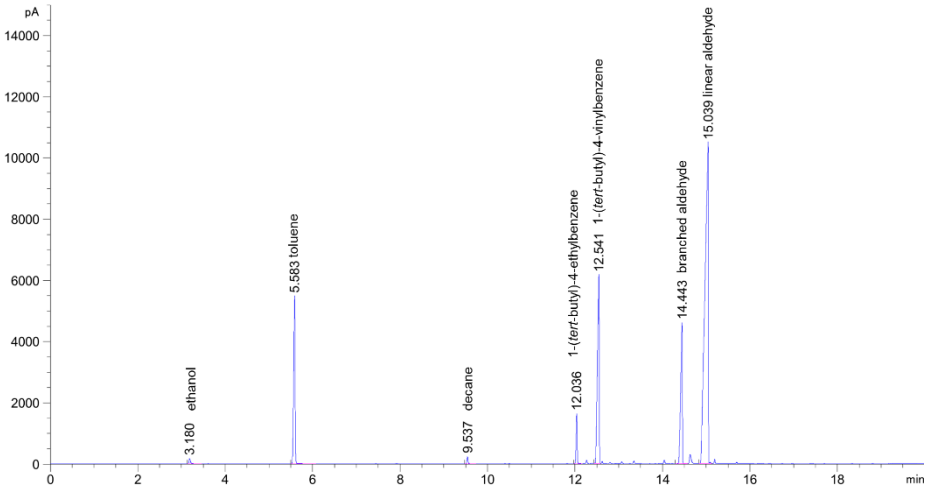

Figure S18. GC of 1-(*tert*-butyl)-4-vinylbenzene hydroformylation

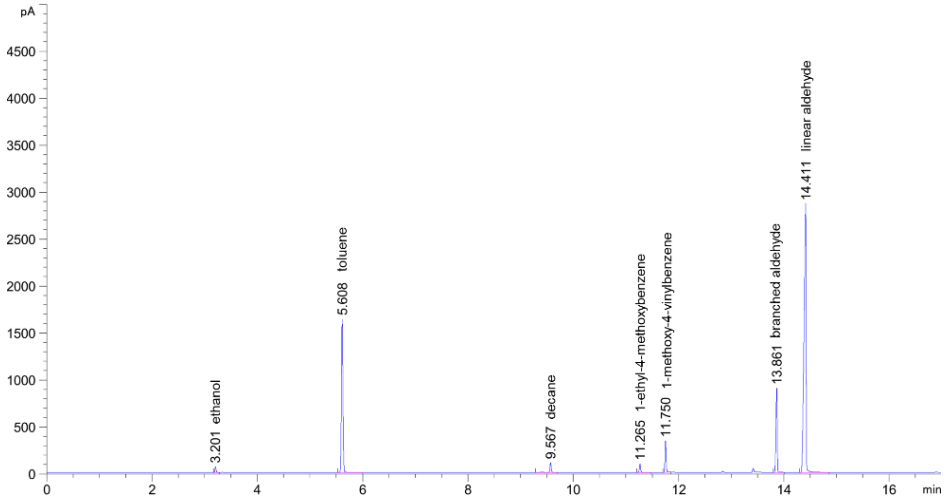

Figure S19. GC of 1-methoxy-4-vinylbenzene hydroformylation

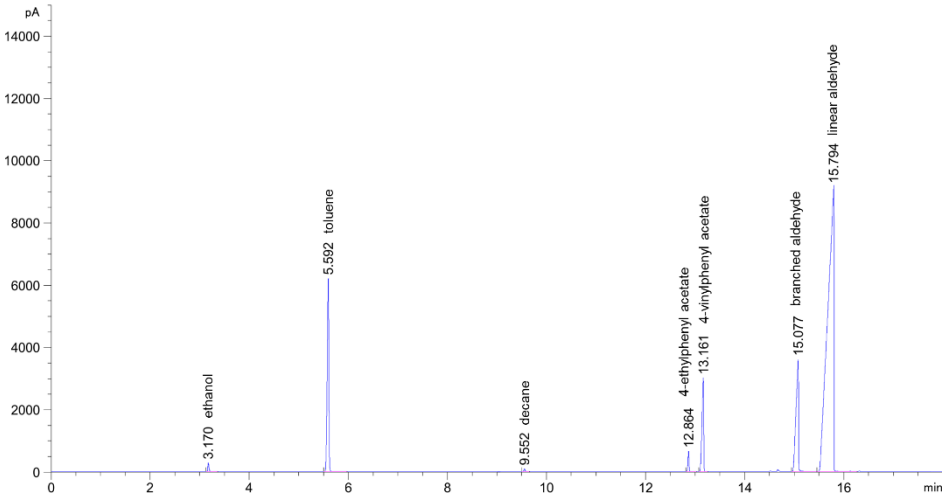

Figure S20. GC of 4-vinylphenyl acetate hydroformylation

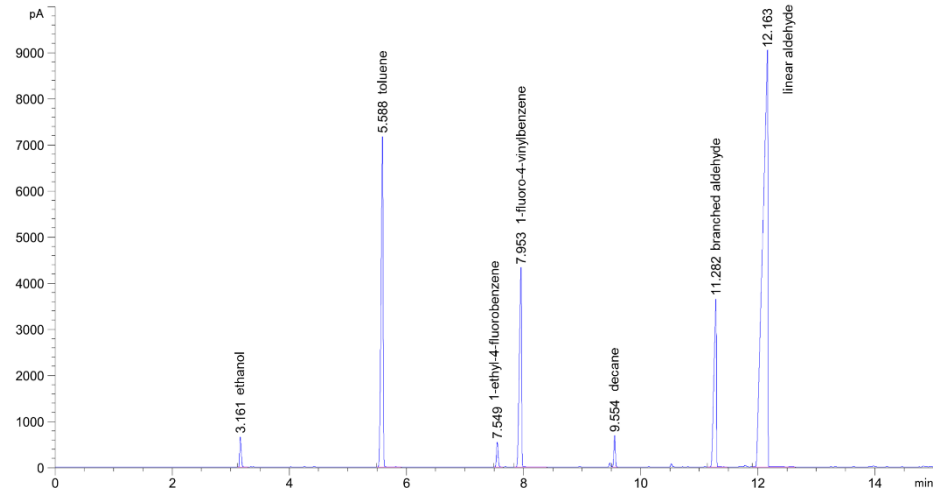

Figure S21. GC of 1-fluoro-4-vinylbenzene hydroformylation

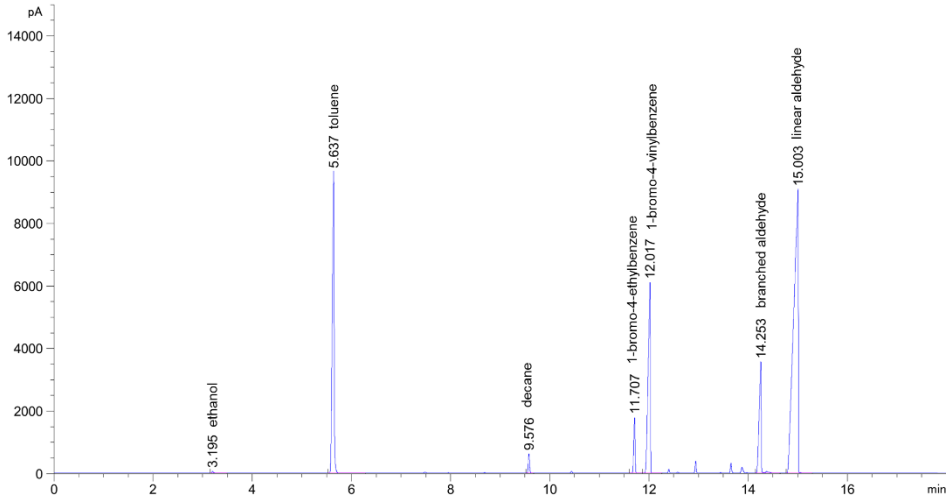

Figure S22. GC of 1-bromo-4-vinylbenzene hydroformylation

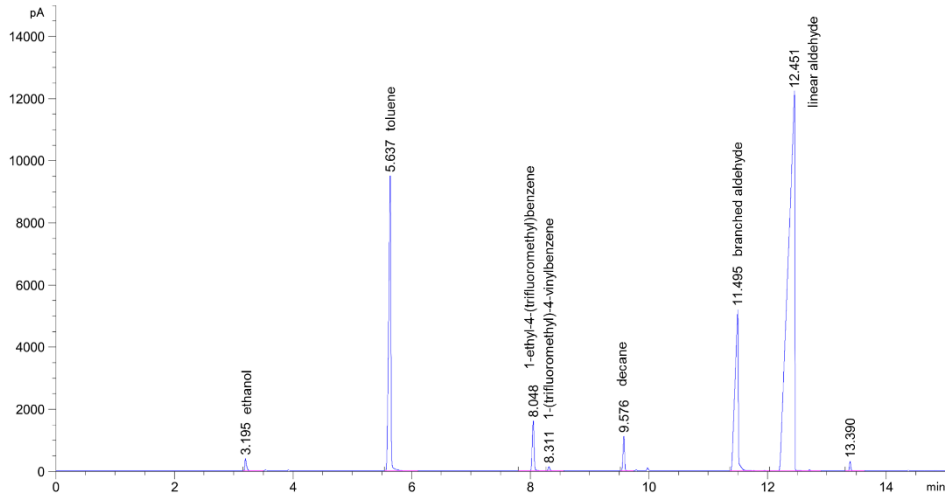

Figure S23. GC of 1-(trifluoromethyl)-4-vinylbenzene hydroformylation

7. Comparison with Relevant Literature

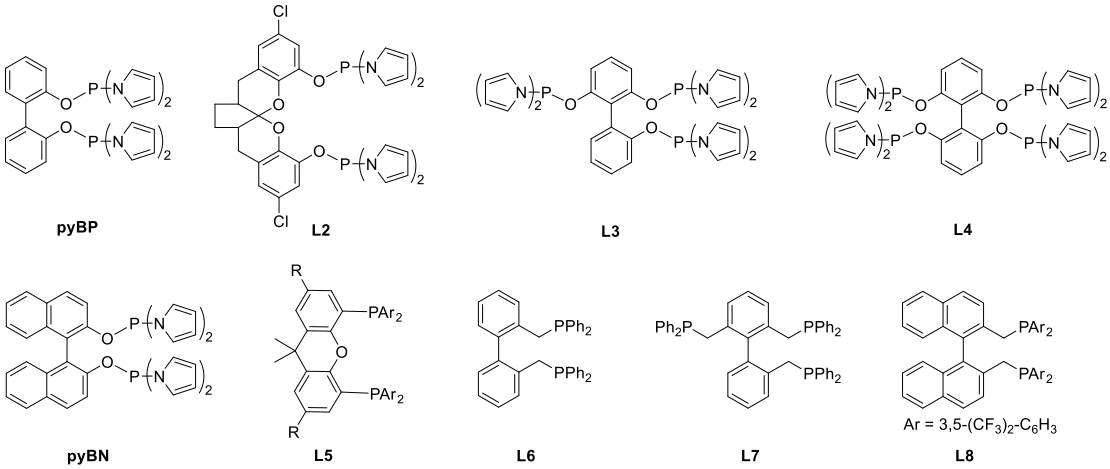

Table S7 Comparison with relevant literature

Substrate	Ligand (Source)	TON	TOF (h^{-1})	Sel.$_{CHO}$ (%)	Sel.$_{ISO}$ (%)	Linear (%)	*l/b*	Reaction Condition
1-hexene	**pyTFBP** (This work)	46700	23350	86.1	12.8	99.8	403	S/C = 50000, L/Rh = 2 2 MPa, 70 °C, 2 h
	pyBP[3] (*Chem. Eur. J.* **2012**, 18, 15288)	9000	/	/	8.7	98.9	86.7	S/C = 10000, L/Rh = 2 4 MPa, 100 °C, 3 h
	L2[3] (*Chem. Eur. J.* **2012**, 18, 15288)	7800	/	/	18	99.4	174.4	S/C = 10000, L/Rh = 2 4 MPa, 100 °C, 3 h
	L3[4] (*Org. Lett*. **2013**, 15, 1048)	7400	/	/	22.3	99.8	471	S/C = 10000, L/Rh = 3 1 MPa, 80 °C, 2 h
	L4[4] (*Org. Lett*. **2013**, 15, 1048)	7500	/	/	24.5	99.8	618	S/C = 10000, L/Rh = 3 1 MPa, 80 °C, 2 h
	L6[5] (*Org. Chem. Front*. **2014**, 1, 947)	9900	/	/	8.1	97.9	47.5	S/C = 10000, L/Rh = 4 1 MPa, 120 °C, 4 h
	L7[5] (*Org. Chem. Front*. **2014**, 1, 947)	9900	/	/	6.9	98.5	66.8	S/C = 10000, L/Rh = 4 1 MPa, 120 °C, 4 h
2-octene	**pyTFBP** (This work)	930	465	77.4	15.4	98.1	51.3	S/C = 1000, L/Rh = 4 2 MPa, 100 °C, 2 h
	pyTFBP (This work)	8360	1672	62.4	26.2	97.8	44.0	S/C = 10000, L/Rh = 24 2 MPa, 100 °C, 5 h
	pyBP[3] (*Chem. Eur. J.* **2012**, 18, 15288)	6600	/	/	/	95.1	19.2	S/C = 10000, L/Rh = 3 1.5 MPa, 110 °C, 15 h
	pyBN[6] (*Chem. Lett*. **2009**, 38, 596)	1126	/	/	/	97.5	39.5	S/C = 1325, L/Rh = 1.5 0.7 MPa, 100 °C, 1 h
	L2[3] (*Chem. Eur. J.* **2012**, 18, 15288)	4500	/	/	/	96.0	24.0	S/C = 10000, L/Rh = 3 1.5 MPa, 110 °C, 15 h
	L3[4] (*Org. Lett*. **2013**, 15, 1048)	2400	/	/	/	98.0	47	S/C = 10000, L/Rh = 3 1 MPa, 100 °C, 2 h
	L4[4] (*Org. Lett*. **2013**, 15, 1048)	2000	/	/	/	98.3	59	S/C = 10000, L/Rh = 3 1 MPa, 100 °C, 2 h
	L5[7]	/	112	/	/	90	9.5	S/C = 637, L/Rh = 10

	(*Adv. Synth. Catal*. **2004**, 346, 789)							0.36 MPa, 120 °C
	L6[5] (*Org. Chem. Front*. **2014**, 1, 947)	1400	/	/	/	84.5	5.5	S/C = 2000, L/Rh = 4 0.5 MPa, 120 °C, 4h
	L7[5] (*Org. Chem. Front*. **2014**, 1, 947)	1400	/	/	/	87.4	7.0	S/C = 2000, L/Rh = 4 0.5 MPa, 120 °C, 4h
	L8[8] (*Angew. Chem. Int. Ed*. **2001**, 40, 3408)	/	319	/	/	86.0	6.1	S/C = 10000, L/Rh = 5 1 MPa, 120 °C, 16h
styrene	**pyTFBP** (This work)	38200	38200	95.5	/	85.8	6.1	S/C = 40000, L/Rh = 3 1 MPa, 100 °C, 1 h
	pyBP[3] (*Chem. Eur. J*. **2012**, 18, 15288)	6900	/	/	/	78.0	3.5	S/C = 10000, L/Rh = 2 1 MPa, 100 °C, 3 h
	pyBN[9] (*Appl. Organometal. Chem*. **2013**, 27, 474)	1000	/	/	/	85.4	5.8	S/C = 1000, L/Rh = 5 1 MPa, 90 °C, 1 h
	L2[3] (*Chem. Eur. J*. **2012**, 18, 15288)	6000	/	/	/	77.5	3.4	S/C = 10000, L/Rh = 2 1 MPa, 100 °C, 3 h
	L3[4] (*Org. Lett*. **2013**, 15, 1048)	/	360	/	/	76.2	3.2	S/C = 1000, L/Rh = 4 1 MPa, 0.5 h
	L4[4] (*Org. Lett*. **2013**, 15, 1048)	/	470	/	/	83.4	5.0	S/C = 1000, L/Rh = 4 1 MPa, 0.5 h
	L5[10] (*Dalton Trans*. **2013**, 42, 137)	/	/	/	/	71	2.5	S/C = 2000, L/Rh = 2 1 MPa, 80 °C

8. DFT Calculation Results for Ligand

All DFT calculations were performed at the B3LYP[11-14]-D3[15]/6-31G(d) level (6-31G(d) basis set for C, H, O, N, P) implemented in the Gaussian 16[16] packages in gas phase. Frequency calculations were performed to confirm that one imaginary frequency for all transition states. To save computational costs, "g09defaults" keyword was used in all calculations.

Geometry optimization results for different conformations

To determine stable conformations for ligand, different conformations were calculated and the results are shown in Table S8-S10. And the most stable conformations of ligands were used as initial geometries for potential energy surface scan.

Table S8. Different conformations of pyBP, 3 kcal/mol less than the most stable conformation, with zero-energy corrected electronic energies and Gibbs free energies. Calculated at B3LYP-D3/6-31+G* level in gas phase at 298.15K.

Entry	Relative electronic energy (kcal/mol)	Relative Gibbs free energy (kcal/mol)	Absolute electronic energy (Hartree)	Absolute Gibbs free energy (Hartree)
a-1	0.0	*0.0*	-2133.157386	-2133.222682
a-2	0.0	*0.0*	-2133.157385	-2133.222671
a-3	0.1	*0.1*	-2133.157228	-2133.222520
a-4	2.2	*0.9*	-2133.153931	-2133.221197

a-5	2.2	*1.4*	-2133.153947	-2133.220514
a-6	1.8	*1.9*	-2133.154571	-2133.219713
a-7	2.8	*1.9*	-2133.152986	-2133.219666
a-8	3.8	*2.0*	-2133.151307	-2133.219444
a-9	1.1	*2.1*	-2133.155638	-2133.219364
a-10	1.1	*2.1*	-2133.155636	-2133.219359
a-11	1.7	*2.3*	-2133.154739	-2133.218964
a-12	1.7	*2.4*	-2133.154622	-2133.218818
a-13	1.2	*2.5*	-2133.155469	-2133.218649
a-14	1.2	*2.5*	-2133.155466	-2133.218639
a-15	2.4	*2.6*	-2133.153638	-2133.218513
a-16	3.6	*2.7*	-2133.151690	-2133.218453
a-17	3.9	*2.7*	-2133.151250	-2133.218434
a-18	2.5	*3.0*	-2133.153414	-2133.217897
a-19	2.5	*3.0*	-2133.153415	-2133.217896

Table S9. Different conformations of pyBN, 3 kcal/mol less than the most stable conformation, with zero-energy corrected electronic energies and Gibbs free energies. Calculated at B3LYP-D3/6-31+G* level in gas phase at 298.15K.

Entry	**Relative electronic energy (kcal/mol)**	**Relative Gibbs free energy (kcal/mol)**	**Absolute electronic energy (Hartree)**	**Absolute Gibbs free energy (Hartree)**
b-1	0.0	*0.0*	-2440.358038	-2440.429591
b-2	0.1	*0.2*	-2440.357914	-2440.429253
b-3	0.4	*0.6*	-2440.357321	-2440.428633
b-4	1.1	*1.2*	-2440.356279	-2440.427732
b-5	0.3	*1.2*	-2440.357605	-2440.427662
b-6	0.7	*1.3*	-2440.357002	-2440.427449
b-7	0.7	*1.4*	-2440.356896	-2440.427417
b-8	3.0	*1.5*	-2440.353258	-2440.427220
b-9	2.7	*1.9*	-2440.353669	-2440.426570
b-10	1.7	*2.0*	-2440.355373	-2440.426389
b-11	2.5	*2.2*	-2440.353990	-2440.426134
b-12	4.7	*2.3*	-2440.350508	-2440.425889
b-13	3.3	*2.4*	-2440.352783	-2440.425697
b-14	2.9	*2.6*	-2440.353433	-2440.425408
b-15	4.4	*2.9*	-2440.351047	-2440.424976
b-16	3.7	*2.9*	-2440.352151	-2440.424962
b-17	3.9	*3.0*	-2440.351807	-2440.424828

Table S10. Different conformations of pyTFBP, 3 kcal/mol less than the most stable conformation, with zero-energy corrected electronic energies and Gibbs free energies. Calculated at B3LYP-D3/6-31+G* level in gas phase at 298.15K.

Entry	Relative electronic energy (kcal/mol)	Relative Gibbs free energy (kcal/mol)	Absolute electronic energy (Hartree)	Absolute Gibbs free energy (Hartree)
c-1	0.0	*0.0*	-2747.944015	-2748.019444
c-2	0.5	*0.3*	-2747.943146	-2748.018997
c-3	0.7	*0.4*	-2747.942910	-2748.018771
c-4	0.7	*1.1*	-2747.942894	-2748.017703
c-5	2.1	*1.3*	-2747.940609	-2748.017343
c-6	1.2	*1.4*	-2747.942077	-2748.017270
c-7	1.2	*1.4*	-2747.942095	-2748.017147
c-8	2.3	*1.6*	-2747.940352	-2748.016914
c-9	2.0	*1.8*	-2747.940892	-2748.016652
c-10	2.9	*1.8*	-2747.939426	-2748.016550
c-11	2.6	*1.8*	-2747.939799	-2748.016533
c-12	3.9	*1.8*	-2747.937780	-2748.016515
c-13	3.2	*1.9*	-2747.938953	-2748.016417
c-14	3.6	*2.1*	-2747.938351	-2748.016111
c-15	2.5	*2.2*	-2747.939979	-2748.015901
c-16	2.5	*2.2*	-2747.939976	-2748.015897
c-17	3.1	*2.2*	-2747.939003	-2748.015865
c-18	3.1	*2.4*	-2747.939015	-2748.015599
c-19	3.4	*2.4*	-2747.938593	-2748.015564
c-20	3.4	*2.4*	-2747.938588	-2748.015563
c-21	4.5	*2.5*	-2747.936909	-2748.015479
c-22	3.3	*2.5*	-2747.938823	-2748.015414
c-23	2.1	*2.6*	-2747.940692	-2748.015347
c-24	2.5	*2.6*	-2747.940002	-2748.015264
c-25	4.9	*2.6*	-2747.936144	-2748.015249
c-26	2.7	*2.6*	-2747.939775	-2748.015244
c-27	5.1	*2.7*	-2747.935925	-2748.015217
c-28	5.0	*2.7*	-2747.936072	-2748.015199
c-29	3.9	*2.7*	-2747.937722	-2748.015116
c-30	3.8	*2.7*	-2747.938000	-2748.015096
c-31	4.1	*2.8*	-2747.937448	-2748.015031
c-32	5.5	*2.8*	-2747.935310	-2748.014989
c-33	3.0	*2.8*	-2747.939230	-2748.014908
c-34	3.5	*2.9*	-2747.938401	-2748.014811
c-35	4.1	*2.9*	-2747.937478	-2748.014775
c-36	4.1	*3.0*	-2747.937499	-2748.014594

Results of relaxed potential energy surface scan around aryl axis with the most stable conformation.

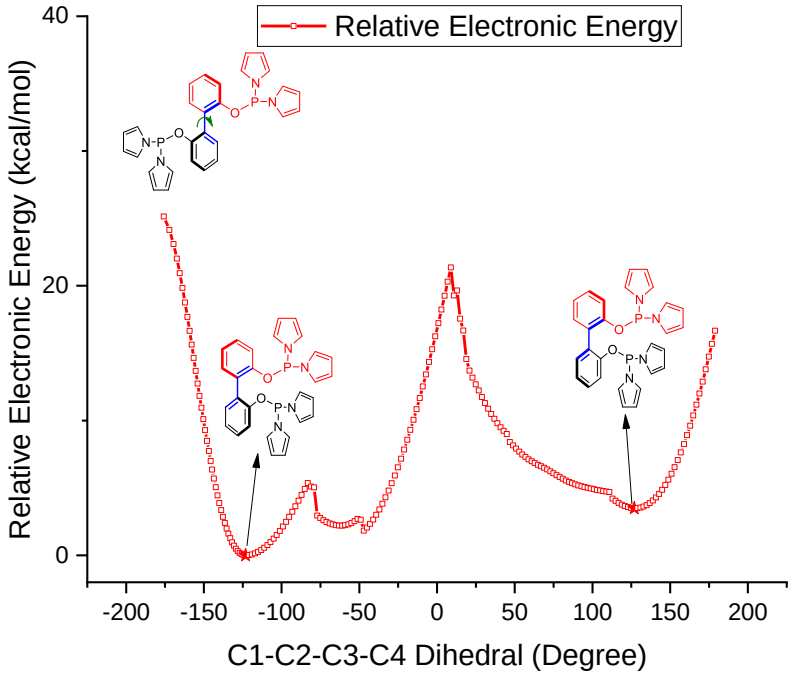

Figure S24. Results of relaxed potential energy surface scan around aryl axis with the most stable conformation of pyBP. with pyBP as the energy refence point. Calculated at B3LYP-D3/6-31+G* level in gas phase at 298.15K.

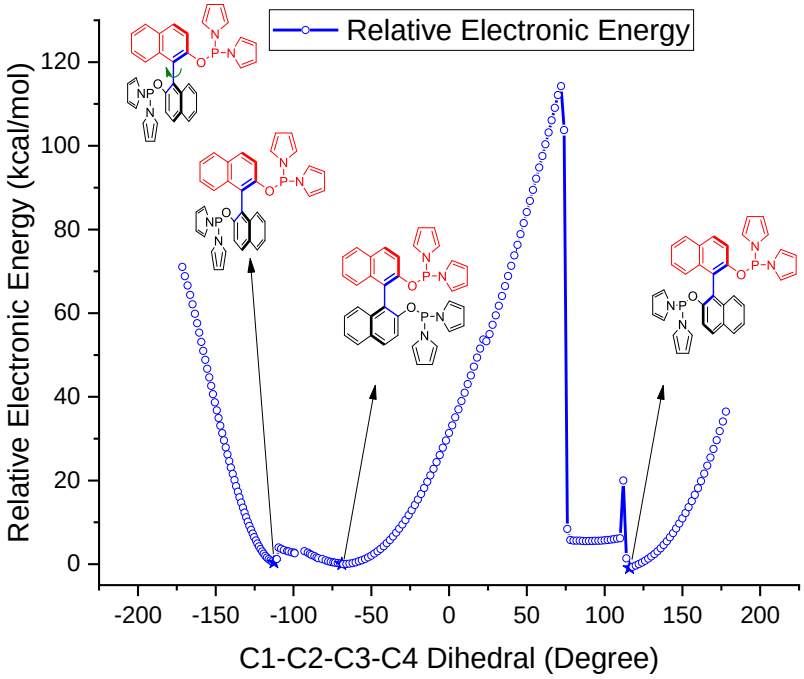

Figure S25. Results of relaxed potential energy surface scan around aryl axis with the most stable conformation of pyBN. with pyBN as the energy refence point. Calculated at B3LYP-D3/6-31+G* level in gas phase at 298.15K.

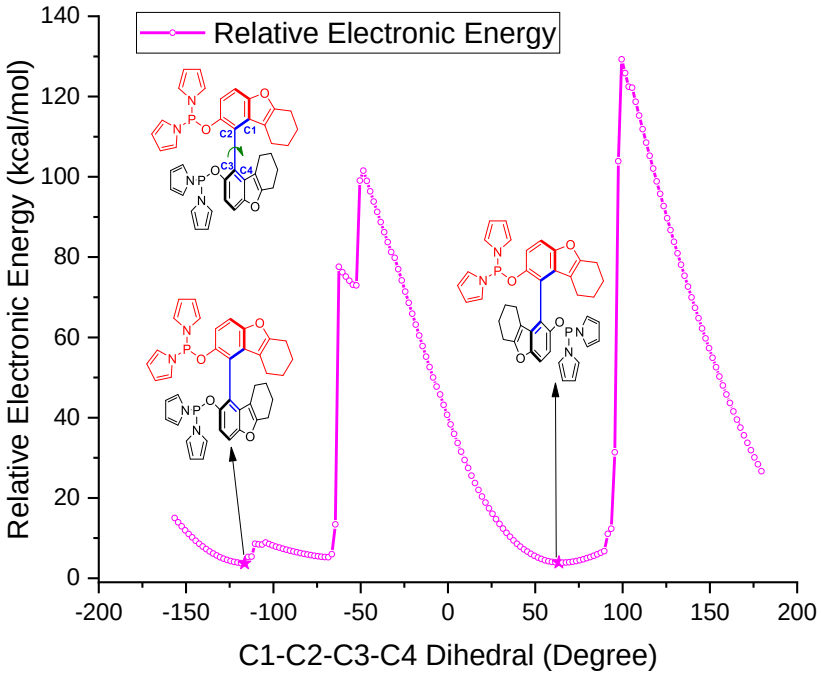

Figure S26. Results of relaxed potential energy surface scan around aryl axis with the most stable conformation of pyTFBP. with pyTFBP as the energy refence point. Calculated at B3LYP-D3/6-31+G* level in gas phase at 298.15K.

9. DFT Calculation Results for Styrene Hydroformylation

All geometry optimizations were performed at the B3LYP[11-14]-D3[15]/6-31G(d)/SDD level (6-31G(d) basis set for C, H, O, N, P; and SDD effective core potential basis set for Rh) implemented in the Gaussian 16[16] packages in gas phase. Frequency calculations were performed to confirm that one imaginary frequency for all transition states, and that zero imaginary frequencies for all intermediates/reactants/products. To save computational costs, "g09defaults" keyword was used in all calculations.

Table S11. Reactants, products, intermediates and transition states for hydroformylation with the Rh catalyst, with zero-energy corrected electronic energies and Gibbs free energies. Calculated at B3LYP-D3/6-31+G* level in gas phase at 298.15K.

Entry	Relative electronic energy (kcal/mol)	Relative Gibbs free energy (kcal/mol)	Absolute electronic energy (Hartree)	Absolute Gibbs free energy (Hartree)
b-P	/	/	-424.034887	-424.069936
l-P	/	/	-424.034020	-424.069873
$PhCHCH_2$	/	/	-309.517022	-309.548727
CO	/	/	-113.301879	-113.321017
H2	/	/	-1.165337	-1.176825
IN-b-1	-20.8	*-6.3*	-3282.092021	-3282.179868
TS-b-1	-12.5	*2.3*	-3282.078867	-3282.166245
IN-b-2	-14.4	*-1.0*	-3282.081830	-3282.171414

IN-b-3	-41.8	*-16.8*	-3395.427369	-3395.517628
TS-b-2	-33.9	*-8.9*	-3395.414793	-3395.505094
IN-b-4	-44.9	*-19.7*	-3395.432263	-3395.522281
IN0	-27.5	*-18.5*	-3085.887616	-3085.971717
IN1	0.0	*0.0*	-2972.541856	-2972.621155
IN-l-1	-22.6	*-7.7*	-3282.094927	-3282.182137
TS-l-1	-14.2	*0.9*	-3282.081496	-3282.168429
IN-l-2	-21.2	*-7.3*	-3282.092697	-3282.181569
IN-l-3	-43.7	*-20.3*	-3395.430390	-3395.523187
TS-l-2	-28.7	*-4.5*	-3395.406441	-3395.498111
IN-l-4	-38.4	*-14.1*	-3395.421967	-3395.513327
TS-l-3	-36.0	*-6.6*	-3396.583525	-3396.678320
IN-l-5	-45.6	*-14.3*	-3396.598689	-3396.690549
IN-l-6	-42.4	*-11.4*	-3396.593723	-3396.685932
TS-l-4	-34.1	*-3.5*	-3396.580358	-3396.673301
IN-l-7	-45.9	*-17.3*	-3396.599197	-3396.695258

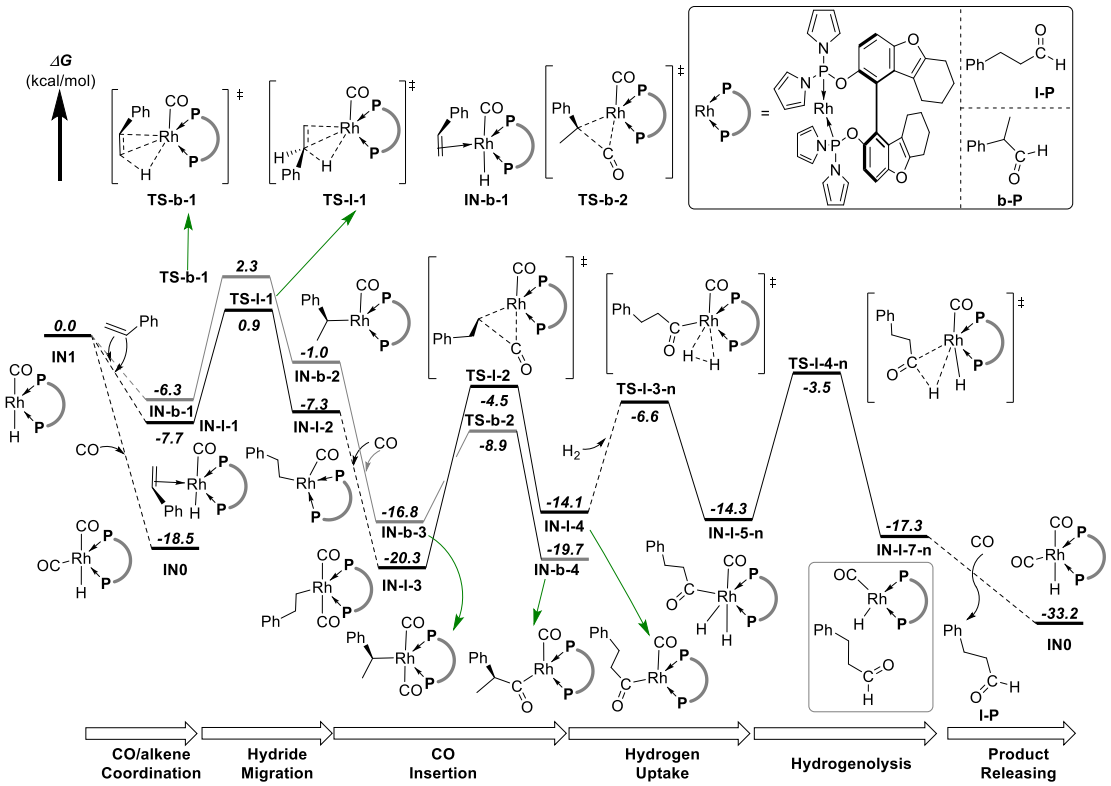

Figure S27. DFT calculation suggested free energy profiles for full reaction pathway for linear styrene hydroformylation to linear product (**l-P**) and partial reaction pathway for branched styrene hydroformylation to branched product (**b-P**), with the hydride migration step as the selectivity determination step. Calculated at B3LYP-D3/6-31+G* level in gas phase at 298.15K.

IN0

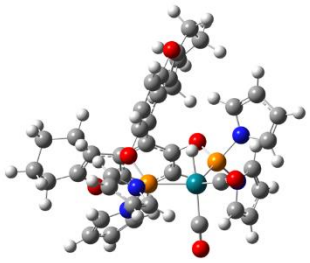

IN1

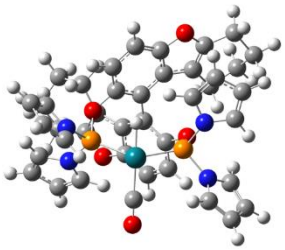

IN-b-1

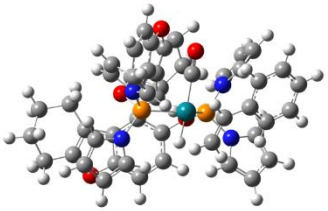

IN-b-2

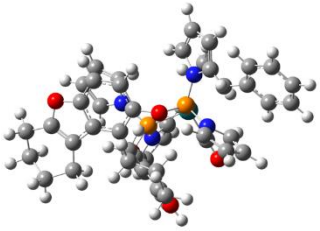

IN-b-3

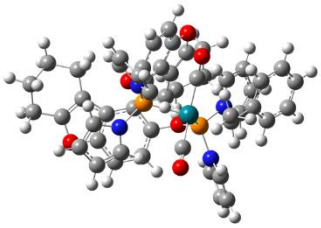

IN-b-4

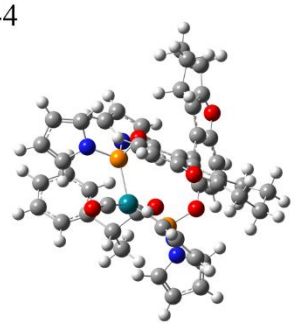

IN-l-1

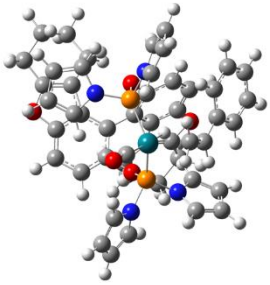

IN-l-2

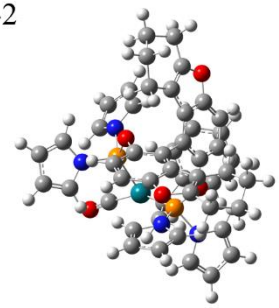

IN-l-3

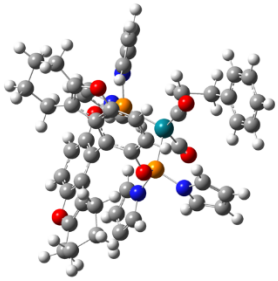

IN-l-4

IN-l-5-n

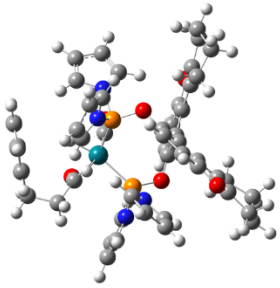

IN-l-6-n

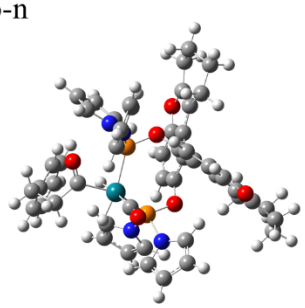

IN-l-7-n

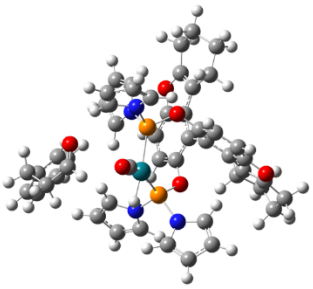

TS-b-1

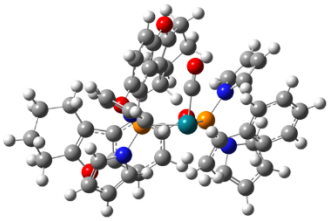

TS-b-2

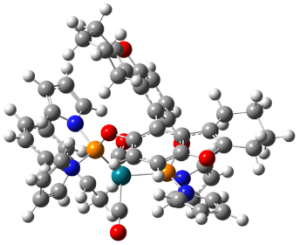

TS-l-1

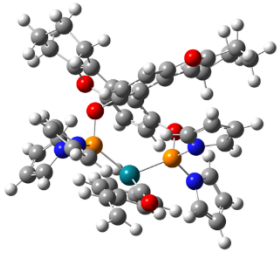

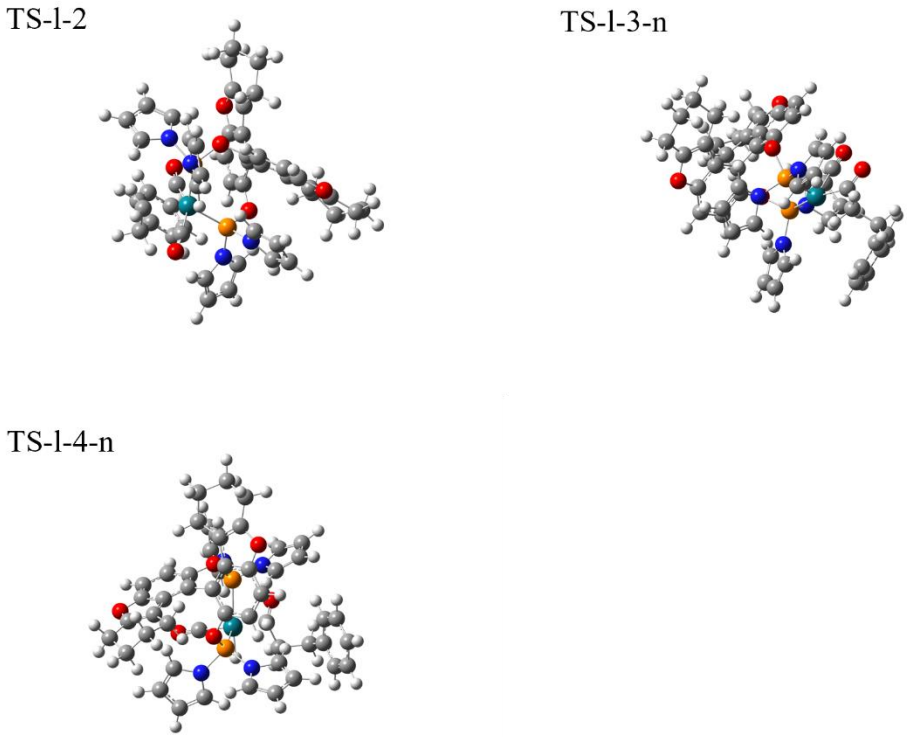

Figure S28. Structures of intermediates or transition states in Figure S27. White, grey, orange, blue, red, and cyan colors refer to hydrogen, carbon, phosphorus, nitrogen, oxygen, and rhodium, respectively.

Table S12. Imaginary frequency for transition states in the reaction pathway. Calculated at B3LYP-D3/6-31G(D) level in gas phase at 298.15K.

Entry	Imaginary frequency (cm^{-1})
TS-b-1	-745.0215i
TS-b-2	-198.4894i
TS-l-1	-581.9416i
TS-l-2	-258.8206i
TS-l-3	-839.1340i
TS-l-4	-613.6967i

10. References

(1) H. Kelgtermans, L. Dobrzanska, L. Van Meervelt and W. Dehaen, *Tetrahedron*, 2011, **67**, 3685.
(2) C. J. Cobley, C. H. Hanson, M. C. Lloyd, S. Simmonds and W. J. Peng, *Org. Proc. Res. Dev*. 2011, **15**, 284.
(3) X. Jia, Z. Wang, C. Xia and K. Ding, *Chem. Eur. J*. 2012, **18**, 15288.
(4) C. Chen, Y. Qiao, H. Geng and X. Zhang, *Org. Lett.*, 2013, **15**, 1048.
(5) C. Chen, P. Li, Z. Hu, H. Wang, H. Zhu, X. Hu, Y. Wang, H. Lv and X. Zhang, *Org. Chem. Front.*, 2014, **1**, 947.
(6) W. Liu, M. Yuan, H. Fu, H. Chen, R. Li and X. Li, *Chem. Lett*., 2009, **38**, 596.
(7) R. P. J. Bronger, J. P. Bermon, J. Herwig, P. C. J. Kamer and P. W. N. M. van Leeuwen, *Adv. Synth. Catal.*, 2004, **346**, 789.
(8) H. Klein, R. Jackstell, K.-D. Wiese, C. Borgmann and M. Beller, *Angew. Chem., Int. Ed.*, 2001, **40**, 3408.
(9) C. Zheng, M. Mo, H. Liang, X. Zheng, H. Fu, M. Yuan, R. Li and H. Chen, *Appl. Organometal. Chem*., 2013, **27**, 474.
(10) E. Boymans, M. Janssen, C. Müller, M. Lutzc and D. Vogt, *Dalton Trans.*, 2013, **42**, 137.
(11) A. D. Becke, *Phys. Rev. A*. 1988, **38**, 3098.
(12) C. Lee, W. Yang and R. G. Parr, *Phys. Rev. B*. 1988, **37**, 785.
(13) A. D. Becke, *J. Chem. Phys*. 1993, **98**, 1372.
(14) P. J. Stephens, F. J. Devlin, C. F. Chabalowski and M. J. Frisch, *J. Phys. Chem*. 1994, **98**, 11623.
(15) S. Grimme, J. Antony, S. Ehrlich and H. Krieg, *J. Chem. Phys*. 2010, **132**, 154104.
(16) M. J. Frisch, G. W. Trucks, H. B. Schlegel, G. E. Scuseria, M. A. Robb, J. R. Cheeseman, G. Scalmani, V. Barone, G. A. Petersson, H. Nakatsuji, X. Li, M. Caricato, A. V. Marenich, J. Bloino, B. G. Janesko, R. Gomperts, B. Mennucci, H. P. Hratchian, J. V. Ortiz, A. F. Izmaylov, J. L. Sonnenberg, Williams, F. Ding, F. Lipparini, F. Egidi, J. Goings, B. Peng, A. Petrone, T. Henderson, D. Ranasinghe, V. G. Zakrzewski, J. Gao, N. Rega, G. Zheng, W. Liang, M. Hada, M. Ehara, K. Toyota, R. Fukuda, J. Hasegawa, M. Ishida, T. Nakajima, Y. Honda, O. Kitao, H. Nakai, T. Vreven, K. Throssell, Jr., J. A. Montgomery, J. E. Peralta, F. Ogliaro, M. J. Bearpark, J. J. Heyd, E. N. Brothers, K. N. Kudin, V. N. Staroverov, T. A. Keith, R. Kobayashi, J. Normand, K. Raghavachari, A. P. Rendell, J. C. Burant, S. S. Iyengar, J. Tomasi, M. Cossi, J. M. Millam, M. Klene, C. Adamo, R. Cammi, J. W. Ochterski, R. L. Martin, K. Morokuma, O. Farkas, J. B. Foresman and D. J. Fox, *Gaussian 16 Rev. B.01*. Wallingford, CT, 2016.